Experimental Evaluation and Image Reconstruction Based Optimization of the Spatially Variant PSF on the Ingenuity TF PET/MR Scanner

Fotis A. Kotasidis, *Member IEEE*, Susanne Heinzer, Habib Zaidi, *Senior Member, IEEE*

Abstract — **The Ingenuity TF PET/MR is a newly developed hybrid scanner combining the molecular imaging capabilities of PET with the excellent soft tissue contrast of MRI. Due to the magnetic field, spatial resolution in PET could potentially be affected. As such, it is important to characterize the system's point spread function (PSF) and understand its variation under spatial transformations to guide clinical studies. An array of 12×7 printed point sources was scanned for 120 minutes to sample the spatially variant PSF with the MR magnet on and the reconstructed data (blob-based LOR-RAMLA) were fitted in image space with a double 3-D Gaussian mixture model to derive parameters of interest. Based on the analysis, the axial resolution was found to be the least variant (up to 5.7mm) followed by the tangential (up to 6.4mm) and the radial (up to 6.9mm). The radial and tangential components were found to be variant under radial transformations and almost invariant under axial transformation. However, this radial dependency was found to be minimal with the resolution degrading only by 2.5mm towards the edge of the radial FOV. Overall the PET subsystem exhibits excellent resolution characteristics mainly due to the fact that the raw data are not under-sampled/re-binned enabling the spatial resolution to be dictated by the scanner's intrinsic resolution and the image reconstruction parameters. To this extent, blob parameters used during image reconstruction could be further optimized to improve the system's resolution characteristics.**

***Index Terms*—PET/MRI, PSF, printed point sources, spatial resolution**

I. Introduction

THE renewed interest in PET/MR imaging during the last few years due to advancements in detector technology has paved the way for leading manufacturers to develop commercial whole body PET/MR systems [1]. The need to avoid mutual interference between the PET and MR components has resulted in different designs amongst the available systems. In integrated PET/MR systems, such as the Siemens mMR, the 2 scanner components acquire simultaneous data within a common FOV [2]. Such an approach requires substantial changes in the hardware technology and mainly in the PET detectors and electronics. On the other hand, one can maintain the technology currently used in PET and MR systems with minimal changes, by combining them in a tandem arrangement, allowing sequential acquisition between the 2 components. One such example is the tri-modality PET/CT–MRI commercialized by General Electric, where the patient is transferred on a dedicated shuttle from one system into the other [3]. The Philips Ingenuity TF PET/MR system uses a rotating patient handling system which enables sequential imaging, allowing fused images to be obtained similar to the design concept of a standard PET/CT system [4]. The system comprises the Gemini TF PET and the Achieva 3T X-series MRI systems (Fig. 1).

In all system designs, the PET detector electronics should not affect the homogeneity of the MR field nor interfere electromagnetically in any way. To avoid such effects while using detectors based on current PET scanner designs on the Ingenuity PET/MR system, the PET detector electronics are removed from the PET gantry and are located outside the Faraday cage. At the same time the magnetic field from the MR can potentially influence the in-plane spatial resolution of the PET due to effects on the electron trajectories in the PMTs. Moreover, the Lorentz force acting on the positrons with a velocity vector component perpendicular to the magnetic field, will cause them to spiral between particle interactions with matter, effectively reducing positron range especially for high energy positron emitting isotopes. In the Ingenuity system, both the distance between the individual

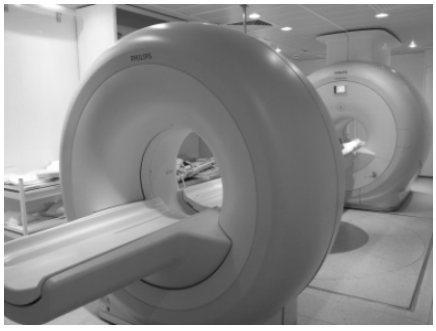

Fig. 1. The Philips Ingenuity TF PET/MR system is based on the Gemini TF PET and the Achieva 3T X-series MRI scanners and uses a rotating patient handling system to allow sequential scanning between the 2 scanners.

F. A. Kotasidis is with the Division of Nuclear Medicine and Molecular Imaging, Geneva University Hospital, CH-1211 Geneva, Switzerland.
Susanne Heinzer is with Philips AG Healthcare, Zurich, Switzerland.
Habib Zaidi is with the Division of Nuclear Medicine and Molecular Imaging, Geneva University Hospital, CH-1211 Geneva, Switzerland and with Geneva Neuroscience Center, Geneva University, Geneva, Switzerland.

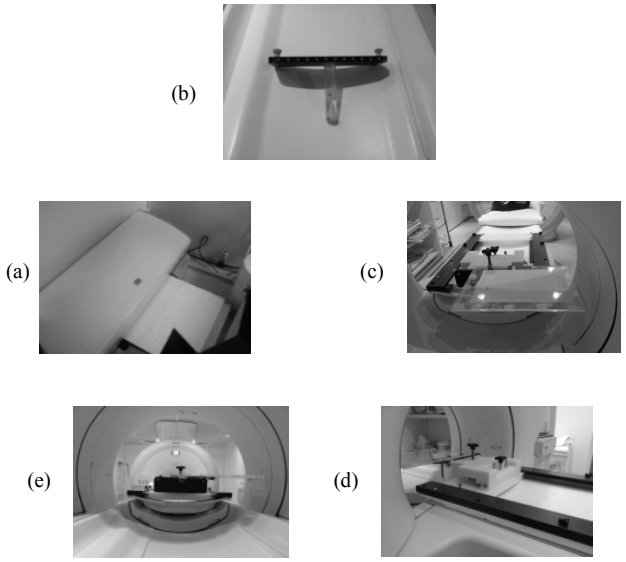

Fig. 2. A printer was used to produce the point source array (a). Holes were drilled on the top of the QC point source holder at 2cm intervals (b) and the Perspex sheets with the point source array were screwed in place (c).The assembly was then attached on the phantom holder which was subsequently attached on the patient handling system with the help of railings (d). The array was positioned horizontally extending from the centre towards the edge of the radial FOV (e).

components (~3m) as well as the additional shielding on the PMTs and detector rings provide sufficient protection against such effects. Nevertheless detailed characterization of the resolution characteristics of the PET scanner under the presence of the MR field is important and could provide valuable information to guide clinical studies where spatial resolution is of importance.

In this work, we investigate the spatial resolution properties of the Ingenuity TF PET/MR scanner by measuring its spatial-variant PSF in image space, using a printed point source array technique and a custom made phantom design. We also report on the PSF asymmetry and its spatial dependency. Furthermore, due to the blob-based reconstruction, an optimization of the blob parameters can be performed to improve its spatial resolution capabilities.

II. METHODS

Measuring the spatially variant PSF experimentally usually requires multiple acquisitions using robotic equipment to accurately position a positron-emitting source at discrete positions throughout the FOV. Whether modeling the resolution characteristics in projection or in image space, rotation and translation symmetries can be taken into account to reduce the locations where the PSF needs to be sampled. Modeling the PSF in image space is less challenging from an experimental setup point of view. The PSFs can be used with a list-mode resolution recovery reconstruction while multiple points can be used to simultaneously sample the PSF at different locations in the FOV [5],[6]. At the same time, due to the parameterization of the measured response and the subsequent interpolation of the parameters in the remaining positions, image-based methods yield similar results to projection-based modeling when used within resolution recovery based image reconstruction algorithms [6].

To produce the point sources, a standard HP printer was used to print multiple radioactive Fluorine-18 point sources on an A4 paper using a predefined template array drawn on Microsoft publisher [6]. Ink (~0.3ml) was mixed with Fluorine-18 (~0.1ml) and the solution was injected into a modified cartridge via a syringe. An array of 12×7 sources in the radial and axial directions, respectively, was printed. The sources were 1mm in diameter and the array covered half the radial FOV (0...27.5 cm) and almost the entire axial FOV (-7.5...7.5 cm). A conservative 2.5 cm point source spacing was used both in the axial and radial directions to avoid any overlap of the reconstructed PSFs. To boost the activity printed, the paper was reprinted 3 times ensuring activity deposition at the same position in each reprint. Since the paper doesn't provide sufficient material for the positrons to annihilate, a Perspex phantom was used for that purpose. A tissue equivalent phantom consisting of 2 Perspex sheets (3 mm thick/sheet), between which the array was placed, was used for positioning and to provide annihilating material (Fig.2).

To place the Perspex sheets in the FOV and allow movements in all degrees of freedom for precise positioning of the sources, the phantom holder used for daily QC of the PET scanner, was modified to accommodate the point source array. Holes were drilled with 2 cm intervals at the top bracket of the QC point source holder and the Perspex sheets were screwed to place, extending from the centre of the radial FOV. Accurate positioning of the array was assisted by the scanner's laser system which although not used for direct alignment, provided a fixed reference frame. Multiple test scans with the array were acquired and reconstructed to locate the centre of the FOV and subsequent adjustments were done with respect to the laser system. Printed guide-lines on the point source array helped the alignment with respect to the reference laser lines. Once in place, PET data were acquired in PET

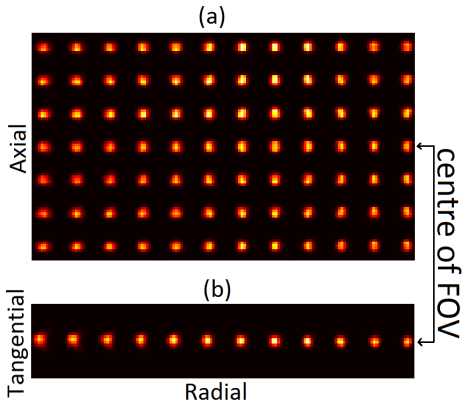

Fig. 3. Axial (a) and transverse (b) slice through the reconstructed point source data. From a qualitative assessment the radial elongation of the kernels is visible towards the edge of the radial FOV.

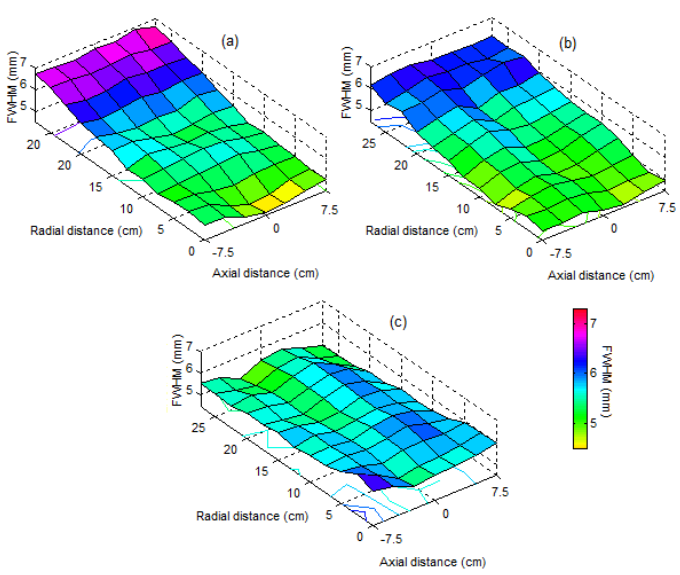

Fig. 4. Parametric surface plots of the radial (a), tangential (b) and axial (c) FWHM as a function of radial and axial distances. The radial and tangential FWHM degrades towards the edge of the radial FOV while the axial FWHM appears to be almost invariant under radial transformations. Furthermore the spatial resolution is invariant under axial transformations in all directions.

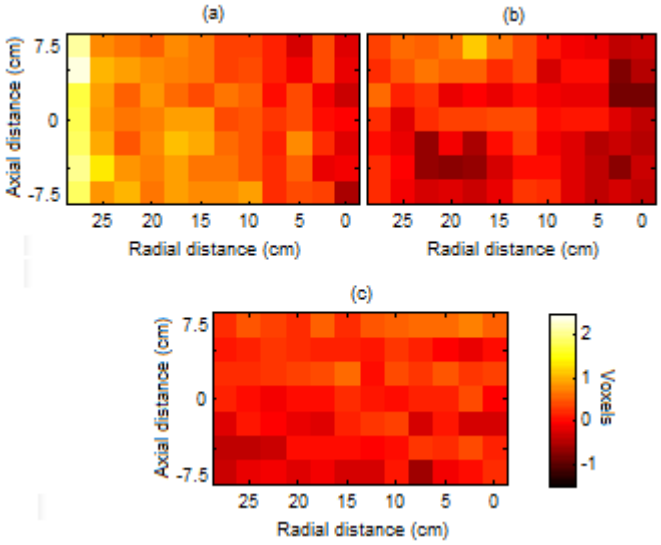

Fig. 5. Parametric images of the radial (a), tangential (b) and axial (c) PSF asymmetry as a function of radial and axial distance. The asymmetry is calculated as the difference between the means of the 2 Gaussian distributions.

only mode (no MR acquisition) with the MR magnet on for 120 minutes to enable high counting statistics data to be collected (~100M prompts). The raw data were reconstructed using standard software provided by the manufacturer (LOR-RAMLA with 10 iterations), using standard blob and relaxation parameters used in clinical protocols. Since the data were acquired in PET only mode, no attenuation correction was used, which is a reasonable assumption since the Perspex sheets result in minimal attenuation. Furthermore since an attenuation map was not readily available, scatter correction was not performed during the reconstruction. The reconstructed data were fitted in image space with a Gaussian mixture model of 2 3-D distributions to estimate 13 parameters (standard deviation and mean with axial, radial and tangential components for each Gaussian as well as a weighting parameter controlling the mixing of the 2 Gaussians).

III. RESULTS

Fig. 3 shows a horizontal (a) and transverse (b) plane through the reconstructed point sources. Looking at the PSFs, the radial elongation of the kernels is visible towards the edge of the radial FOV while the axial resolution appears to be invariable going from one side of the axial FOV to the other. The quantitative analysis reveals similar findings (Fig. 4) where parametric surface plots of the radial (a), tangential (b) and axial (c) FWHM are shown for all the point sources and as a function of axial and radial distances from the centre of the FOV. The worst resolution properties are seen in the radial direction, followed by the tangential and the axial. The radial resolution fluctuates from ~4.7 mm in the centre of the radial FOV (r=0, z=0) to ~6.9 mm at the edge of the radial FOV (r=27.5 cm, z=0) with the array tangentially centered. Furthermore, the radial resolution appears to be almost axially independent with a small axial variation mainly close to the centre of the radial FOV, with the FWHM going from ~4.7 mm at the centre (r=0, z=0) to 5 mm at the 2 ends of the axial FOV (r=0, z= ±7.5 cm). The tangential resolution follows a similar trend as a function of the radial distance with ~4.7 mm and ~6.4 mm at the centre (r=0, z=0) and edge (r=27.5 cm, z=0) of radial FOV. Finally, the axial resolution appears to be relatively constant throughout the FOV with the FWHM being invariant under radial and axial transformations compared to the radial and tangential, with small fluctuations (maximum difference ~1mm). Similar surface plots can be obtained for each of the 13 parameters fitted to each kernel in order to assess their spatial dependency. By using a double Gaussian to fit the data, the PSF asymmetry can be evaluated, as the means of the 2 distributions are free to be fitted by the data, thus allowing the radial dependency of the radial elongation to be assessed. In Fig. 5 the radial, tangential and axial PSF asymmetry is plotted, which is derived as the difference in the respective means between the 2 Gaussian distributions. As expected, the asymmetry is heavily pronounced in the radial direction and increases towards the edge of the radial FOV due to the parallax error. This is due to the fact that as the PSF becomes more elongated the radial displacement between the 2 Gaussians tends to increase in order to model the data. On the other hand, no significant asymmetry was observed in the axial and tangential directions as there are no detector related effects to cause such an elongation in the respective directions.

Finally, the 2 parametric maps of the weighting proportion between the 2 Gaussian distributions are shown in Fig. 6, with the 2 weights for each respective pixel in the maps summing

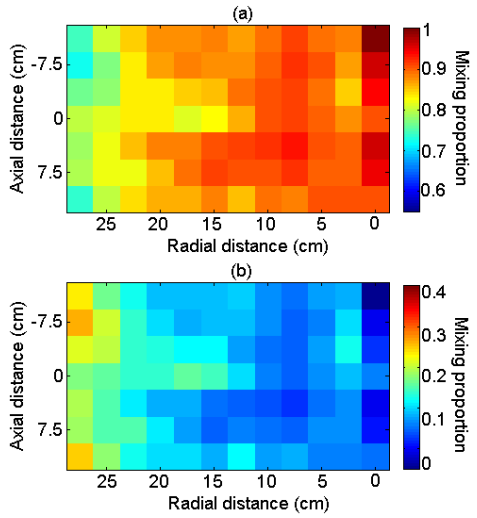

Fig. 6. Parametric images of the mixing proportion between the 2 3-D Gaussian distribution used to fit each individual Kernel.

up to unity. Fig 6(a) is the proportion of the 1st Gaussian which accounts for the main fast decaying part of the kernel and as can be seen, close to the centre of the radial FOV accounts for most of the distribution. This is due to the fact that the kernels close to the centre of the radial FOV being free from any parallax error effects are normally distributed and can be modeled even by a single Gaussian distribution. Going towards the edge of the FOV the distributions become asymmetric and as such the 2nd Gaussian distribution begins to model the elongated tails with the mixing proportion increasing as the tails account for more in the overall kernel.

IV. Discussion & Conclusion

In this work we experimentally measured the spatially variant PSF on the Ingenuity TF PET/MR. Such PSF measurements could potentially be used within a resolution modeling image reconstruction. All the acquisitions were performed with the MR magnet on, while no MR data were acquired for attenuation correction as the phantom would give a void signal. Previous work reported that the spatial resolution characteristics were comparable with MR magnet on and off and almost similar to the PET subsystem mounted on a combined PET-CT scanner, which is indicative of the effectiveness of magnetic shielding and overall system design [4]. The axial resolution was found to vary minimally in contrast to previous measurements in which the axial resolution appears to vary substantially as a function of radial distance [6]. Also the radial and tangential resolution increases only by ~2.5 mm towards the edge of the radial FOV which again results only in a small degradation. These characteristics can be attributed to the fact that the scanner is using LOR-based reconstruction in which no axial under-sampling (span), angular mashing and radial interpolation (arc correction) is used during data acquisition and preprocessing, compared to systems which use data reduction techniques to speed up reconstruction and minimize data storage at the expense of reduced spatial resolution. As such, using a spatially invariant as opposed to a spatially variant kernel within a resolution recovery image reconstruction algorithm may be a valid approximation. This is true as the gains from using a spatially variant PSF in a whole body scanner where the spatial resolution varies only by 2.5 mm due to parallax error could be small to justify the additional computational load and variable convergence rate at different locations in the image due the variable size of the kernel. In the results presented in this work, we used standard blob parameters and with these set to balance the SNR and resolution characteristics. An optimization procedure is underway to evaluate different blob parameters and their effect on the system's spatially variant resolution characteristics [7].

Acknowledgements

This work was supported by the Swiss National Science Foundation under grant SNSF 31003A-135576.

References

[1] H. Zaidi.and A. D. Guerra, "An outlook on future design of hybrid PET/MRI systems, " Medical Physics, 38 (10), pp. 5667-5689, 2011.
[2] G. Delso, S. Furst, B. Jakoby, R. Ladebeck,C. Ganter, SG. Nekolla, M. Schwaiger, SI. Ziegler, " Performance measurements of the Siemens mMR integrated whole-body PET/MR scanner, ".J Nucl Med Vol 52(12), pp 1914–1922, 2011
[3] P. Veit-Haibach, F.P. Kuhn, F. Wiesinger, G. Delso and G. von Schulthess, "PET-MR imaging using a Tri-modality PET/CT – MR system with a dedicated shuttle in clinical routine, " Magn. Reson. Mater. Phy, Biol. Med., Special issue: "MRI and PET together: friends or foes" MAGMA. 2012.
[4] H. Zaidi, N. Ojha , M. Morich, J. Griesmer, Z. Hu, P. Maniawski, O. Ratib, D.Izquierdo-Garcia, ZA. Fayad, L. Shao, "Design and performance evaluation of a whole-body Ingenuity TF PET–MRI system, " Phys. Med Biol vol 56, pp. 3091–3106, 2011.
[5] C. Cloquet, F. C. Sureau, M. Defrise, G.Van Simaeys, N. Trotta and S. Goldman , "Non-Gaussian space-variant resolution modelling for list-mode reconstruction, " Phys. Med. Biol. Vol 55, pp 5045-5066, 2010
[6] F.A. Kotasidis, J. C. Matthews, G. I. Angelis, P. J. Noonan, A. Jackson, P. Price, W. R. Lionheart, A. J. Reader, "Single scan parameterization of space variant point spread functions in image space via a printed array: Impact for two PET/CT scanners,"Phys. Med. Biol. vol. 56, pp. 2917–2942, 2011.
[7] S. Matej and R. M. Lewitt, "Practical considerations for 3-D image reconstruction using spherically symmetric volume elements, " IEEE Trans Med Imaging, vol. 15, pp. 68-78, 1996.